Asian Journal of Chemistry; Vol. 34, No. 6 (2022), 1465-1471

ASIAN JOURNAL OF CHEMISTRY

https://doi.org/10.14233/ajchem.2022.23631

Removal of Copper(II) Ion using Nanochitosan/Carboxymethyl Cellulose/Grapheme Oxide Composite Biosorbent

S. SUGASHINI[1], T. GOMATHI[1,*], S. PAVITHRA[1], P.N. SUDHA[1,*], J. ANNIE KAMALA FLORENCE[2] and A. MUBASHIRUNNISA[3]

[1]Biomaterials Research Lab, PG and Research Department of Chemistry, D.K.M. College for Women, Vellore-632001, India
[2]Department of Chemistry, Voorhees College, Vellore-632001, India
[3]Department of Chemistry, Sri Krishna College of Engineering, Arakkonam-631003, India

*Corresponding authors: E-mail: drparsu8@gmail.com; drgoms1@gmail.com

Received: 24 November 2021; *Accepted*: 26 February 2022; *Published online*: 18 May 2022; AJC-20807

The present study aimed to prepare a novel biosorbent of nanochitosan (NCS)/carboxymethyl cellulose (CMC)/graphene oxide (GO) and used to remove Cu(II) ion from wastewater system. The prepared nanocomposite was characterized using FTIR, XRD and SEM analysis. The FTIR and XRD results revealed the formation of novel NCS/CMC/GO nanocomposite. Rough surface morphology of nanocomposite was confirmed from the SEM analysis results. The removal efficiency of Cu(II) ion was evaluated through batch mode by varying pH, adsorbent dose, contact time and initial metal ion concentration. The maximum removal of Cu(II) ion was 80.1% at pH 4, 92.4% at 360 min contact time and about 89.2% for 3 g adsorbent dose. Theoretical models such as Langmuir isotherm, Freundlich isotherm, and kinetics models were used to evaluate the experimental results. After examining, the results revealed that the adsorption follows Freundlich isotherm and pseudo-second-order models. The adsorption capacity of the prepared nanocomposite was 145.22 mg/g.

Keywords: Ternary composite, carboxymethyl cellulose, Graphene oxide, Nanochitosan, Batch adsorption.

INTRODUCTION

Toxic heavy metal ion pollution had become today's one of the most severe environmental problems issue. Owing to the augmented urbanization and substantial industrialization activity, huge amounts of toxic organic or inorganic pollutants are released regularly into water resources [1]. Being non-biodegradable, especially the toxic heavy metal ions are most biologically dangerous. They will aggregate in living tissues, thereby undermining human well-being and marine biological systems; hence, its discharge as effluent should be controlled [2,3]. An assortment of the advanced treatment process and procedures were proposed and used to dispose of heavy metals from contaminated water. Many treatment technologies were introduced by several researchers and among them, the adsorption method was found to be the most efficient one [4,5]. When the biomaterials are used for the adsorption process, adsorption can be termed biosorption. For biosorption, numerous agro- and marine wastes were used. Activated carbon [6], biopolymer [7-9] and fly ash [10,11] were used as good adsorbents.

Among the various biopolymers, chitosan with -NH_2 and -OH functional groups have high binding potential towards metal ions, thereby widespread use as a good biosorbent for treating wastewater [12,13]. According to the literature, it was reported that biosorption using chitosan was through chelate formation, which mainly depends on the pH of the metal ion solution. This excessive sensitivity of chitosan to pH can make it gel or dissolvable [14]. Hence, to overcome such challenges, the modification of chitosan is required. It can be done chemically or physically through blending and cross-linking using glyoxal, formaldehyde, glutaraldehyde, isocyanates [15-17], and sodium tripolyphosphate as cross-linking agents to develop the properties of chitosan.

Chitosan nanoparticles are generally prepared by the simple cross-linking method and widely used in fields including pharmaceutical, water treatment, sensors, packaging materials and catalyst due to its nano-size, large surface area and biocompatibility [18,19]. Hence, based on the literature survey in the research work, it aimed to prepare nanochitosan by ionotropic gelation technique and is considered one of the components

in preparing the suitable adsorbent for heavy metal removal. The elimination of Pb(II) ions using nanochitosan has been studied by Zareie *et al*. [20]. Reported results indicate that the nanochitosan has a remarkable elimination capacity of Pb(II) ions even in multiple concentrations than other reported works.

Carboxymethyl cellulose (CMC) is another important, primarily used biopolymer with several wastewater treatment applications, dye removal, drug reduction, drug formulation, papers, plastics and construction [20], since it has a high viscosity, non-toxic and non-allergenic nature. The -OH and -CH_2COOH groups are water-binding in nature and hence it has gained importance because of their sorption properties, high water content, good biodegradability and has broad applications [21,22]. Wang *et al*. [23] reported using CMC-based macroporous material to effectively eliminate Pb^{2+} and Cd^{2+} ions with excellent reusability through five adsorption-desorption cycles.

Graphene oxide (GO), a two-dimensional nanomaterial, can be synthesized by graphite oxidation. The functionalized GO will have OH, COOH, C=O, and epoxide groups on its basal planes and sheet edges [24], thereby possessing higher surface area, chemical stability, excellent electrical and thermal capacity. This functionality makes GO an attractive material to eliminate toxic metals from wastewater even though it is difficult to separate and retrieve after treatment because of its good dispersion property. Graphene-based biosorbent with date syrup has high adsorption capacity and good recyclability for treating methyl violet, Congo red dyes and heavy metals, particularly lead and cadmium [18].

A huge volume of work on the elimination of harmful Cu(II) ions even in low concentrations by different adsorbents is accessible in literature [25-30]. Copper is also a highly toxic heavy metal, in humans, it leads to neurotoxicity disease and hence its expulsion from industrial wastewater turn into necessary. Accordingly, it is advantageous to examine the coordinated adsorption of the two metals and assess the impedance of metal with the adsorption of others. Thus, based on the literature survey, Cu(II) ions were selected to learn biosorption impedance. In the present study, nanochitosan (NCS)/carboxymethyl cellulose (CMC)/graphene oxide (GO) nanocomposite was aimed to prepare and used for the removal of copper ions from the aqueous solution through batch adsorption mode. The parameters such as pH, contact time, adsorption dose and initial metal ion concentrations were varied. The experimental data was evaluated theoretically using Langmuir isotherm, Freundlich isotherm and kinetics models to determine the adsorption efficiency of the prepared blend.

EXPERIMENTAL

Chitosan with a deacetylation degree of 92% was acquired from India Sea Foods, Kerala state, India. The chemicals used in this study, such as sodium tripolyphosphate, were procured from Finar chemicals, India. The analytical grade reagents were utilized in this work.

Preparation of nanochitosan: Ionotropic gelation technique was utilized in this present study to synthesize nanochitosan in dilute solution from chitosan by using sodium tripolyphosphate as a crosslinking agent. Chitosan (1 g) was dissolved in 100 mL of 2% acetic acid. Subsequently, TPP solution (0.8 g in 107 mL of deionized water) was added slowly under magnetic stirring. The milky emulsion followed by suspension of nanochitosan was formed after stirring for about 30 min. The formed suspension was allowed to settle for about 24 h to reach equilibrium. The supernatant solution was decanted and nanochitosan was used for further process.

Preparation of graphene oxide (GO): Functionalization of graphite was done by following the Hummer's method [31]. Graphite (1 g) and $NaNO_3$ (0.5 g) were dissolved using 50 mL of cold H_2SO_4 (cooled underwater bath until it reaches an ice-cold condition of 0 ºC. The mixture is kept stirring for 30 min. For further oxidation to the above mixture, about 4 g of $KMnO_4$ was slowly added under constant stirring. During the addition of $KMnO_4$, the temperature was maintained below 20 ºC. The reaction mixture's temperature was again reduced to ice-cold condition by keeping the beaker in the ice bath for about 1 h. The rate of addition of the $KMnO_4$ was carefully done slowly with control. The ice bath was then removed and allowed the reaction to proceed by stirring the solution under 35 ºC under magnetic stirring for 0.5 h. To this mixture, 50 mL of deionized water was added slowly. The reaction was then continued for 20 min at 98 ºC and followed by 200 mL of deionized water, and 5 mL of H_2O_2 (30%) was added to remove the residual $KMnO_4$ and MnO_2. The resulting mixture was then filtered and washed with DD water and 5% HCl solution (50 mL) for the final purification of graphite oxide. Finally, after filtration and drying under a vacuum at 70 ºC, the GO was obtained as a powder.

Preparation of nanochitosan/carboxylmethyl cellulose/graphene oxide (1:1:0.1) ternary blend: Ternary blend of NCS/CMC/GO was prepared to mix the solutions of nanochitosan (1 g), CMC (1 g) and GO (0.1 g) disseminated in water and well-stirred at 500 rpm for 60 min and followed by that the drying was done for 24 h.

Batch adsorption studies: The evaluation of adsorption ability towards Cu(II) ion using NCS/CMC/GO nanocomposite, 100 mg/mL copper solution was prepared and used. About 0.1809 g of copper sulfate was taken and made up to 1000 mL using deionized water. Copper metal solution (50 mL of 100 ppm) was taken for the experiment. The parameters such as pH (2 to 7), contact time (1 to 6 h), adsorbent dose (1.0, 1.5, 2.0, 2.5 and 3.0 g/50 mL) and metal ion concentration (125 ppm to 1000 ppm/L) were varied and adsorption was studied through batch mode in an orbital shaker at 200 rpm at room temperature. Adsorbed metal ion concentration was analyzed in AAS.

The q_e (metal uptake capacity) can be calculated using the following equation:

$$q_e = \frac{C_i - C_e}{M} \times V$$

where C_i and C_e = initial and equilibrium concentrations, V = volume of the solution in L; M = mass of the adsorbent (g).

The percent adsorption is a calculation using the equation:

$$\text{Adsorption (\%)} = \frac{C_i - C_e}{C_e} \times 100$$

RESULTS AND DISCUSSION

FTIR studies: In present study, using FT-IR [KBr pellet model Shimadzu spectrometer (4000-400 cm^{-1})], the functional groups and their interaction present in the prepared NCS/CMC/GO ternary composites were determined. The FTIR spectra of prepared nanochitosan, NCS/CMC/GO ternary composite before adsorption and NCS/CMC/GO ternary composite after adsorption of Cu(II) ion is shown in Fig. 1. The FT-IR spectrum of nanochitosan (Fig. 1a) shows an absorption band at around 3429 cm^{-1} for -OH stretching in alcohols and NH stretching in amines. Compared with pure chitosan (spectrum not given), the shift in absorption band from 3531 cm^{-1} related to -NH and -OH stretching of chitosan to 3429 cm^{-1} in case of nanochitosan indicates its formation through crosslinking of TPP. Mainly, the band's appearance at 1082 cm^{-1} for P=O stretching vibration of crosslinked TPP with chitosan exhibits nanochitosan formation [31]. To this nanochitosan, CMC/GO was added to prepare NCS/CMC/GO ternary nanocomposite. While adding CMC/GO to NCS (Fig. 1b), the major absorption bands at 3450, 1633, 1419 and 1082 cm^{-1} owing to -OH, C=O, -CH_2 and -CO functional group, respectively increase over nanochitosan matrix. These bands' increased intensity confirmed the CMC's addition and GO onto nanochitosan.

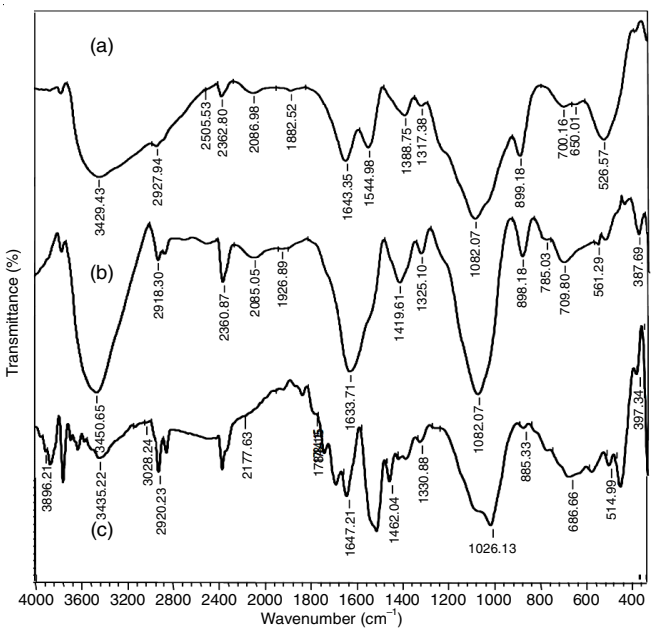

Fig. 1. FTIR spectra of (a) nanochitosan, (b) NCS/CMC/GO ternary nanocomposite, (c) Cu(II) adsorbed NCS/CMC/GO ternary nanocomposite

The FT-IR spectrum of NCS/CMC/GO nanocomposite after Cu(II) ion adsorption is shown in Fig. 1c. From the FTIR spectrum of metal adsorption nanocomposite (Fig. 1c), the adsorption of metal ions onto prepared nanocomposites was confirmed from the shift in band positions and the appearance of new M-L bonds. The bands present at 3435 cm^{-1} for the primary functional groups of nanochitosan (-OH and -NH), CMC (-OH groups) and GO (-COOH and -OH groups); the reduction in the broadness represents the contribution of these groups in M-L bond formation. The lone pair of electrons present in the O and N atoms plays a major role in dative bond formation while removing the heavy metals from the wastewater. These observations successfully lead to the confirmation of metal ion adsorption onto the prepared nanocomposite.

XRD diffraction studies: The crystalline and amorphous phases of the prepared NCS/CMC/GO composite were determined using XRD studies (Shimadzu XD-D1 having Ni-filtered Cu Kα X-ray radiation). The XRD patterns of NCS/CMC/GO composite is displayed in Fig. 2. It displays the diffraction pattern with characteristic peaks at 2θ = 27.40º. The interaction between the three components is mainly through H-bonding and non-covalent interactions, which was confirmed from the broad pattern obtained [32].

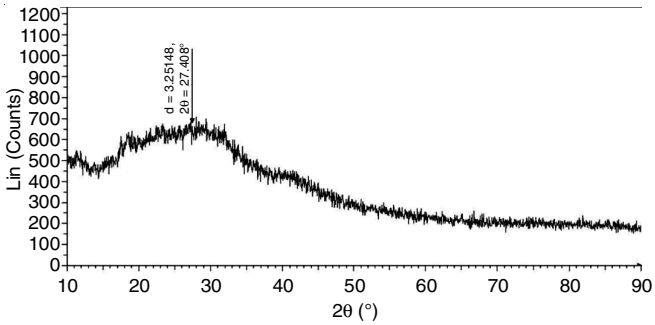

Fig. 2. XRD pattern of NCS/CMC/GO nanocomposites

SEM analysis: The surface morphology of the prepared NCS/CMC/GO ternary nanocomposite was studied using SEM analysis (TESCAN VEGA3 SBH) to find the suitability of the nanocomposite as an adsorbent. Fig. 3 shows the SEM image of the prepared NCS/CMC/GO ternary nanocomposite. The SEM image exhibits a rough surface with a porous structure, which was expected to be a suitable adsorbent for the adsorption process.

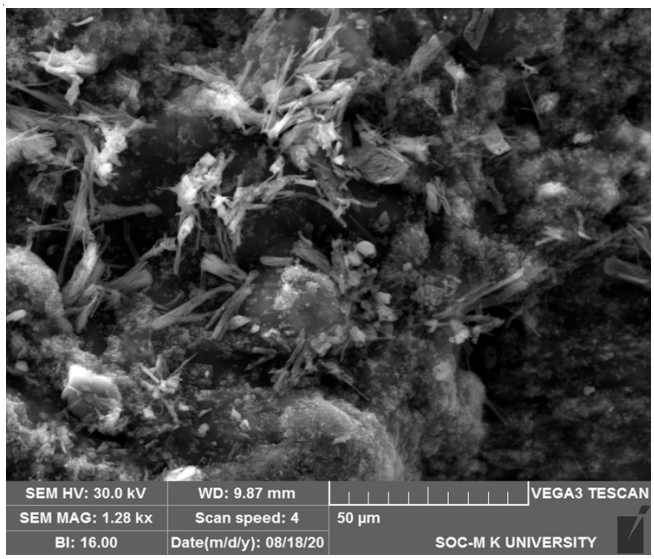

Fig. 3. SEM image of NCS/CMC/GO nanocomposite

EDAX studies: The removal efficiency of the prepared NCS/CMC/GO ternary nanocomposite towards Cu(II) ions was confirmed through EDAX. Fig. 4 shows that Cu(II) ions were adsorbed on the exterior of the adsorbent. The adsorbent's great surface morphology speaks to the adsorption measure's appropriateness through functional groups exposed from the spectra.

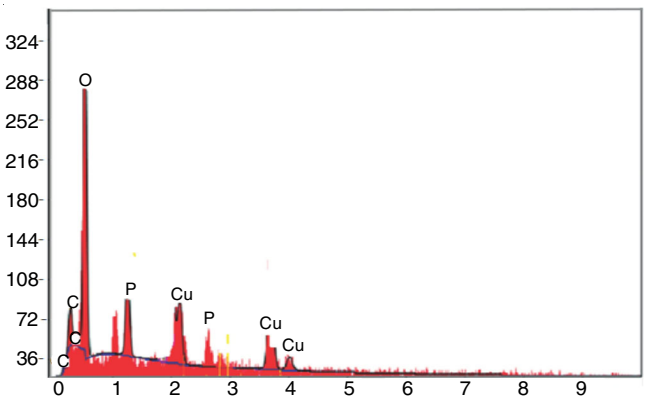

Fig. 4. EDAX spectrum of Cu(II) ion removal using NCS/CMC/GO nanocomposite

Batch adsorption studies: The copper ion's competitive removal by a prepared ternary nanocomposite through batch adsorption was studied by altering pH, contact time, dose and initial metal ion.

Effect of pH: The role of H^+ ions was determined by changing the pH from 2.0 to 9.033, by utilizing the NCS/CMC/GO ternary nanocomposite as an adsorbent at room temperature (Fig. 5a) [33]. It was evident that the percentage removal of toxic copper metal ions increases with pH, reaching optimum at 4 and then descends. At low pH, the H_3O^+ ions were firmly connected with the adsorbent's surface, which renders repulsion to the metal ions for adsorption. But the increased deprotonation was observed while increasing the pH from 2 to 4, thereby decreasing the contact of hydronium ion concentration and adsorbent. This decrease leads to the increased affinity of metal ions towards the adsorbent. It tends to remove copper ions [34,35].

Furthermore, while increasing the pH above neutral, the precipitation was the dominant process than adsorption [36]. From the obtained results, it was concluded that the copper removal was more by NCS/CMC/GO ternary composite at pH 4 and the percentage removal was observed to be 80.1%. On increasing the pH further, the adsorption tends to decrease which is due to the formation of hydroxyl complexes.

Effect of contact time: By keeping the constant pH 4, adsorbent dose (1 g) and initial metal ion concentration (100 ppm), variation of adsorption efficiency with contact time from

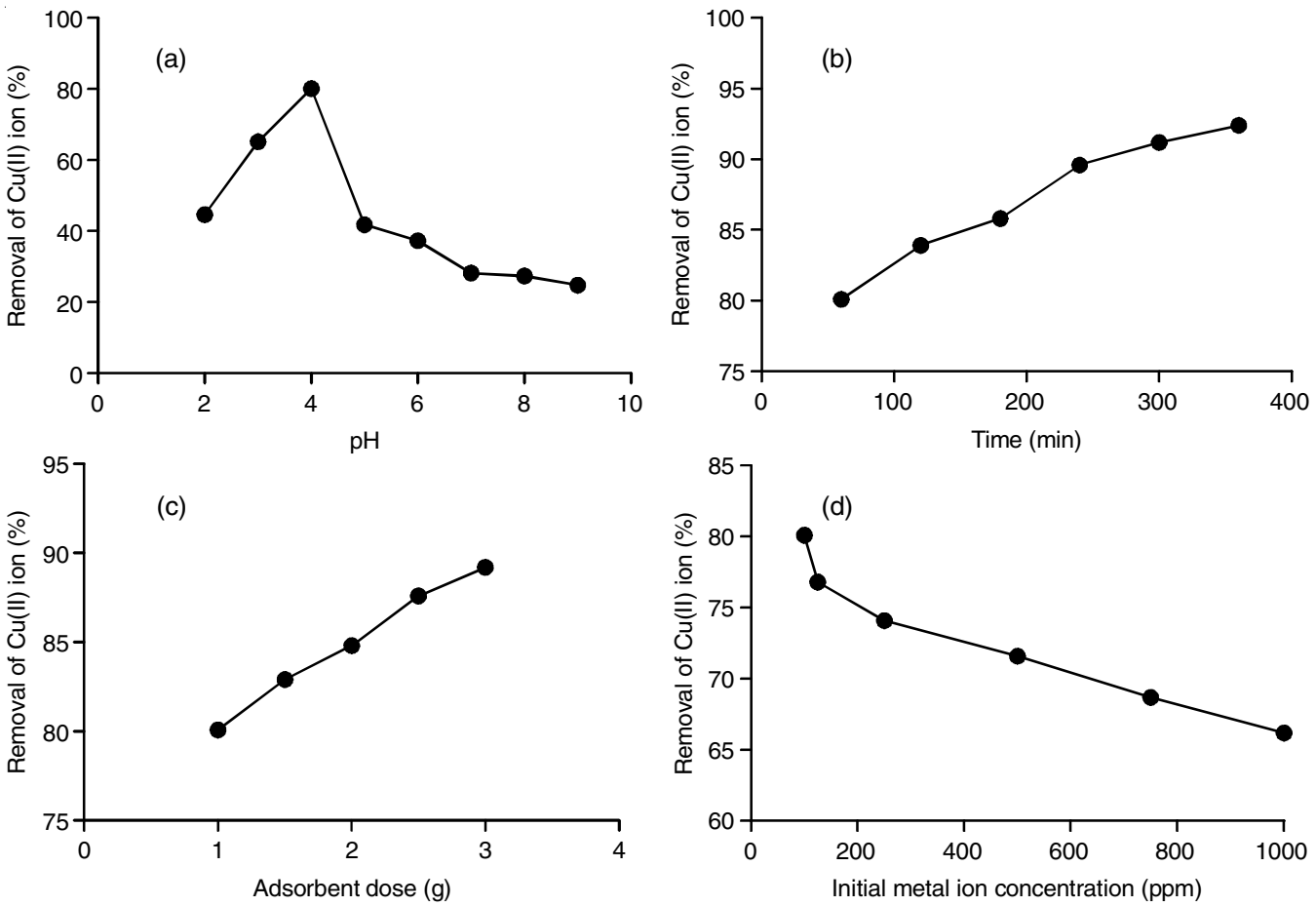

Fig. 5. Batch adsorption analysis - Effect of pH (a), contact time (b), adsorbent dose (c), and initial metal ion concentration (d) on the percentage removal

TABLE-1
LANGMUIR AND FREUNDLICH ISOTHERM PARAMETERS

Langmuir constant				Freundlich constant		
K_L (dm^3/g)	b (dm^3/mg)	C_{max} (mg/g)	R^2	K_f	N	R^2
0.3632	0.002686	145.2265	0.9391	0.7571	1.2970	0.9981

1 to 6 h was monitored (Fig. 5b). On increasing the contact time, the accessibility of metal ions onto the adsorbent increased, thereby enhancing the discharge ability. Henceforth, it reaches saturation on further increment in contact time, thus equilibrium was reached. The achieved result clearly indicates that the prepared ternary nanocomposite's removal efficiency increases with an increase in contact time.

Effect of adsorbent dose: The effect of the prepared NCS/CMC/GO nanocomposite dose for eliminating copper ions was evaluated by varying it from 1 g to 3 g with 0.5 g increments. The prepared NCS/CMC/GO nanocomposite's removal efficiency was increased gradually with increasing the adsorbent concentration (Fig. 5c). Owing to the more significant and huge number of active site accessibility increments in the adsorbent segment that resulted in the strong interaction of Cu(II) ions with NCS/CMC/GO nanocomposite leads to increased removal percentage [37,38]. As soon as the optimum adsorbent dose value reached, because of saturation, the adsorption capacity was reduced [39].

Effect of initial metal ion: The role of metal ion concentration determines the adsorption viability of prepared NCS/CMC/GO nanocomposite. By changing concentration from 1000, 750, 500, 250, and 125 mg/L of copper ions at pH 4, 1 g of adsorbent dose, 1 h of contact time, room temperature consistent the removal percentage was determined. The results revealed that at lower concentrations, all-metal ions will interact with functional groups of the nanocomposite, thereby removing the Cu(II) ions more effectively. The decrease in the removal percentage was observed by increasing the initial metal ion concentration (Fig. 5d). This decrease in percentage removal was due to the absence of adequate surface area for metal ion fixation increments because of the saturation of adsorption sites [40].

Adsorption isotherms: The most commonly used experimental isotherm models are Freundlich and Langmuir models [40].

Freundlich isotherm: The adsorption behaviour of the prepared adsorbent was evaluated using the Freundlich isotherm model, which exhibits a heterogeneous surface favorable for adsorption. The Freundlich equation is given as:

$$\log q_e = \log K_f + \frac{1}{n}\log C_e$$

where K_f = adsorption capacity (Freundlich constant); 1/n = adsorption intensity.

Langmuir isotherm: The Langmuir model is given by

$$\frac{C_{eq}}{C_{ads}} = \frac{bC_{eq}}{K_L} + \frac{1}{K_L}$$

$$C_{max} = \frac{K_L}{b}$$

where C_{ads} = amount of metal ion adsorbed (mg g^{-1}); C_{eq} = equilibrium concentration of remaining metal ion in solution (mg dm^{-3}); K_L = Langmuir constant (dm^3 g^{-1}); b = Langmuir constant (dm^3 mg^{-1}); C_{max} = maximum metal ion to adsorbed onto 1 g adsorbent (mg g^{-1}).

The isotherms parameters values are given in Table-1. For the equilibrium adsorption of Cu(II) ion by the prepared NCS/CMC/GO ternary nanocomposite, the results revealed the fitness of the Freundlich model over the Langmuir model with higher R^2 values (R^2 = 0.9944) signifying heterogeneous adsorption of Cu(II) metal ion. Generally, the smaller the size, easy the penetration will be to reach the active sites. Therefore, resulting in a strong diffusion mechanism that controls metals' transfer to the adsorbent's surface [21]. The higher R^2 values (Table-1) in Freundlich evident that the adsorption Cu(II) ions onto NCS/CMC/GO ternary composite follows multilayer adsorption. The calculated R_L values are given in Table-2 and the results exhibit the adsorption process favourably for $0 < R_L < 1$ [41]. The comparative adsorption capacity of the chitosan based adsorbent towards the removal of Cu ions are shown in Table-3. On reviewing and comparing, it was observed that prepared NCS/CMC/GO ternary composite in this study showed high adsorption capacity.

TABLE-2
R_L VALUE BASED ON LANGMUIR ISOTHERM

Initial concentration (C_i) (mg/L)	Final concentration (C_f) (mg/L)	R_L values
1000	338	0.524145
750	234.75	0.613294
500	142.0	0.723897
250	64.75	0.851848
125	29.0	0.927735
100	20.0	0.949019

Kinetic studies: To facilitate the interaction mechanism between Cu(II) metal ion and NCS/CMC/GO ternary blend, the Lagrangen kinetic models were evaluated [42,43].

A linearized Lagrangen pseudo-first-order model is represented as:

$$\log(q_e - q_t) = \log q_e - \frac{k_1 t}{2.303}$$

The pseudo-second-order rate equation can be represented as follows:

$$\frac{t}{q_t} = \frac{1}{k_2 q_e^2} + \frac{t}{q_e}$$

where q_e and q_t = amounts of metal adsorbed (mg g^{-1}) at equilibrium and at time t (min), respectively; k_1 (min^{-1}) = adsorption rate constant of pseudo-first-order; k_2 (g mg^{-1} min^{-1}) = adsorption rate constant of pseudo-second-order.

TABLE-3
COMPARATIVE TABLE OF C_{max} VALUE FOR THE REMOVAL OF Cu(II) IONS BY REPORTED CHITOSAN BASED ADSORBENTS

Adsorbent	C_{max} values	Ref
Chitin, Chitosan and Chitosan-EDTA	Chitin = 58 Chitosan = 67 Chitosan EDTA = 110	[44]
Chitosan-coated sludge (CCS)	18.83	[45]
Chitosan-*g*-maliec anhydride-*g*-ethylene dimethacrylate	86.95	[46]
Chitosan nanopartilces/bentonite/alginate	1.013	[47]
Nanochitosan/sodium alginate/microcrystalline cellulose beads	43.32	[48]
Salicylaldehyde functionalized chitosan nanoparticles	101.01	[49]
Graphene oxide encapsulated carboxymethylcellulose-alginate hydrogel microspheres	73.27	[50]
Carboxymethyl cellulose/polyacrylamide composite hydrogel	99.01	[51]
Chitosan-GLA beads; Chitosan-alginate beads	Chitosan-GLA bead = 64.62, Chitosan Alginate beads = 67.66	[52]

TABLE-4
KINETICS STUDIES PARAMETERS FOR THE REMOVAL OF Cu(II) IONS

Pseudo first order			Exp. value	Pseudo second order		
q_e (mg/g)	K_1	R^2	q_e (mg/g)	q_e (mg/g)	K_2	R^2
0.184975	0.010225	0.9747	89.464	93.19664	0.000787	0.9997

To analyze the copper ion adsorption kinetics using NCS/CMC/GO nanocomposite, Lagergren mathematical modeling was used to fit contact time data. From the models, the adsorption of copper ion obeys pseudo-second-order model with higher R^2 values than pseudo-first-order kinetics revealed its applicability. The theoretical q_e values were also close to experimental q_e values of pseudo-second-order kinetics, confirming the pseudo-second-order kinetic model (Table-4).

Conclusion

The present study appends the nanochitosan (NCS)/carboxymethyl cellulose (CMC)/graphene oxide (GO) ternary nanocomposite's removal efficiency in an aqueous phase. The prepared nanocomposite was characterized before and after the adsorption of Cu(II) ions using FTIR and SEM-EDAX. The results revealed that NCS/CMC/GO nanocomposite acts as a good biosorbent with greater affinity towards Cu(II) ions through multilayer adsorption processes. The overall results revealed that the prepared NCS/CMC/GO nanocomposite exhibits its efficiency in removing Cu(II) ions. This proves the synergistic effect of all the polymers used to prepare NCS/CMC/GO nanocomposite.

ACKNOWLEDGEMENTS

The authors SS, TG, SP, PNS acknowledge the support given by the DST-FIST lab and the Management of D.K.M. College for Women (Autonomous), Vellore, India.

CONFLICT OF INTEREST

The authors declare that there is no conflict of interests regarding the publication of this article.

REFERENCES

1. S. Khan, A. Achazhiyath Edathil and F. Banat, *Sci. Rep.*, **9**, 18106 (2019); https://doi.org/10.1038/s41598-019-54597-x
2. P. Roccaro, M. Sgroi, and F.G.A. Vagliasindi, *Chem. Eng. Trans.*, **32**, 505 (2013); https://doi.org/10.3303/CET1332085
3. N. Ariffin, M.M.A.B. Abdullah, M.R.R. Mohd Arif Zainol, M.F. Murshed and M.A. Hariz-Zain, Faris, and R. Bayuaji, *MATEC Web Conf.*, **97**, 01023 (2017); https://doi.org/10.1051/matecconf/20179701023
4. S. Elabbas, L. Mandi, F. Berrekhis, M.N. Pons, J.P. Leclerc and N. Ouazzani, *J. Environ. Manage.*, **166**, 589 (2016); https://doi.org/10.1016/j.jenvman.2015.11.012
5. K.S. Bharathi and S.T. Ramesh, *Appl. Water Sci.*, **3**, 773 (2013); https://doi.org/10.1007/s13201-013-0117-y
6. J.M. Dias, M.C.M. Alvim-Ferraz, M.F. Almeida, J. Rivera-Utrilla and M. Sánchez-Polo, *J. Environ. Manage.*, **85**, 833 (2007); https://doi.org/10.1016/j.jenvman.2007.07.031
7. N.K. Lazaridis, G.Z. Kyzas, A.A. Vassiliou and D.N. Bikiaris, *Langmuir*, **23**, 7634 (2007); https://doi.org/10.1021/la700423j
8. T. Gotoh, K. Matsushima and K.-I. Kikuchi, *Chemosphere*, **55**, 135 (2004); https://doi.org/10.1016/j.chemosphere.2003.11.016
9. S. Mondal, *Environ. Eng. Sci.*, **25**, 383 (2008); https://doi.org/10.1089/ees.2007.0049
10. A. Ahmad, R. Ghufran and W.M. Faizal, *Clean Soil Air Water*, **38**, 153 (2010); https://doi.org/10.1002/clen.200900202
11. X. Cui, S. Fang, Y. Yao, T. Li, Q. Ni, X. Yang and Z. He, *Sci. Total Environ.*, **562**, 517 (2016); https://doi.org/10.1016/j.scitotenv.2016.03.248
12. B. Liu, X. Chen, H. Zheng, Y. Wang, Y. Sun, C. Zhao and S. Zhang, *Carbohydr. Polym.*, **181**, 327 (2018); https://doi.org/10.1016/j.carbpol.2017.10.089
13. Z. Yu, Q. Dang, C. Liu, D. Cha, H. Zhang, W. Zhu, Q. Zhang and B. Fan, *Carbohydr. Polym.*, **172**, 28 (2017); https://doi.org/10.1016/j.carbpol.2017.05.039
14. M.-S. Chiou, P.-Y. Ho and H.-Y. Li, *Dyes Pigments*, **60**, 69 (2004); https://doi.org/10.1016/S0143-7208(03)00140-2
15. W.S. Wan Ngah, L.C. Teong and M.A.K.M. Hanafiah, *Carbohydr. Polym.*, **83**, 1446 (2011); https://doi.org/10.1016/j.carbpol.2010.11.004
16. F. Lu and D. Astruc, *Coord. Chem. Rev.*, **356**, 147 (2018); https://doi.org/10.1016/j.ccr.2017.11.003
17. B. Doshi, A. Ayati, B. Tanhaei, E. Repo and M. Sillanpää, *Carbohydr. Polym.*, **197**, 586 (2018); https://doi.org/10.1016/j.carbpol.2018.06.032

18. Y.H. Khan, A. Islam, A. Sarwar, N. Gull, S.M. Khan, M.A. Munawar, S. Zia, A. Sabir, M. Shafiq and T. Jamil, *Carbohydr. Polym.*, **146**, 131 (2016); https://doi.org/10.1016/j.carbpol.2016.03.031
19. J. Safari, Z. Abedi-Jazini, Z. Zarnegar and M. Sadeghi, *Catal. Commun.*, **77**, 108 (2016); https://doi.org/10.1016/j.catcom.2016.01.007
20. C. Zareie, S. Kholghi-Eshkalak, G. Najafpour-Darzi, M.S. Baei, H. Younesi and S. Ramakrishna, *Coatings*, **9**, 862 (2019); https://doi.org/10.3390/coatings9120862
21. H. Nie, M. Liu, F. Zhan and M. Guo, *Carbohydr. Polym.*, **58**, 185 (2004); https://doi.org/10.1016/j.carbpol.2004.06.035
22. D.R. Biswal and R.P. Singh, *Carbohydr. Polym.*, **57**, 379 (2004); https://doi.org/10.1016/j.carbpol.2004.04.020
23. F. Wang, Y. Zhu, H. Xu and A. Wang, *Front Chem.*, **7**, 603 (2019); https://doi.org/10.3389/fchem.2019.00603
24. H. Yang, J.-S. Li and X. Zeng, *ACS Appl. Nano Mater.*, **1**, 2763 (2018); https://doi.org/10.1021/acsanm.8b00405
25. N. Van Vinh, M. Zafar, S.K. Behera and H.-S. Park, *Int. J. Environ. Sci. Technol.*, **12**, 1283 (2015); https://doi.org/10.1007/s13762-014-0507-1
26. P. Manoj Kumar Reddy, K. Krushnamurty, S.K. Mahammadunnisa, A. Dayamani and C. Subrahmanyam, *Int. J. Environ. Sci. Technol.*, **12**, 1363 (2015); https://doi.org/10.1007/s13762-014-0506-2
27. M. Ghasemi, N. Ghasemi, G. Zahedi, S.R.W. Alwi, M. Goodarzi and H. Javadian, *Int. J. Environ. Sci. Technol.*, **11**, 1835 (2014); https://doi.org/10.1007/s13762-014-0617-9
28. G. Mahajan and D. Sud, *J. Environ. Chem. Eng.*, **1**, 1020 (2013); https://doi.org/10.1016/j.jece.2013.08.013
29. T.A.H. Nguyen, H.H. Ngo, W.S. Guo, J. Zhang, S. Liang, Q.Y. Yue, Q. Li and T.V. Nguyen, *Bioresour. Technol.*, **148**, 574 (2013); https://doi.org/10.1016/j.biortech.2013.08.124
30. Y.-H. Li, S. Wang, Z. Luan, J. Ding, C. Xu and D. Wu, *Carbon N.Y.*, **41**, 1057 (2003); https://doi.org/10.1016/S0008-6223(02)00440-2
31. D.C. Marcano, D.V. Kosynkin, J.M. Berlin, A. Sinitskii, A. Slesarev, Z. Sun, L.B. Alemany, W. Lu and J.M. Tour, *ACS Nano*, **4**, 4806 (2010); https://doi.org/10.1021/nn1006368
32. K. Fung, R. Li and S. Tjong, *J. Appl. Polym. Sci.*, **85**, 169 (2002); https://doi.org/10.1002/app.10584
33. H. Deng, L. Yang, G. Tao and J. Dai, *J. Hazard. Mater.*, **166**, 1514 (2009); https://doi.org/10.1016/j.jhazmat.2008.12.080
34. S.A. Ghanem and D.S. Mikkelsen, *Soil Sci.*, **146**, 15 (1988); https://doi.org/10.1097/00010694-198807000-00003
35. J. Ocreto, C.I. Go, J.C. Chua, C.J. Apacible and A. Vilando, *MATEC Web Conf.*, **268**, 6021 (2019); https://doi.org/10.1051/matecconf/201926806021
36. A. Itodo, H. Itodo and M. Gafar, *J. Appl. Sci. Environ. Manag.*, **14**, 1 (2011); https://doi.org/10.4314/jasem.v14i4.63287
37. A.E. Ofomaja and Y.S. Ho, *Dyes Pigments*, **74**, 60 (2007); https://doi.org/10.1016/j.dyepig.2006.01.014
38. D. Uzunoglu, N. Gürel, N. Özkaya and A. Özer, *Desalination Water Treat.*, **52**, 1514 (2014); https://doi.org/10.1080/19443994.2013.789403
39. X.-Y. Huang, X.-Y. Mao, H.-T. Bu, X.-Y. Yu, G.-B. Jiang and M.-H. Zeng, *Carbohydr. Res.*, **346**, 1232 (2011); https://doi.org/10.1016/j.carres.2011.04.012
40. M. Makesmawari, T. Santhi and P. Aswini, *Int. J. Adv. Res. (Indore)*, **4**, 542 (2016).
41. T. Hajeeth, P.N. Sudha, K. Vijayalakshmi and T. Gomathi, *Int. J. Biol. Macromol.*, **66**, 295 (2014); https://doi.org/10.1016/j.ijbiomac.2014.02.027
42. H.-Y. Zhu, Y.-Q. Fu, R. Jiang, J. Yao, L. Xiao and G.-M. Zeng, *Bioresour. Technol.*, **105**, 24 (2012); https://doi.org/10.1016/j.biortech.2011.11.057
43. R. Lakshmipathy and N.C. Sarada, *Desalination Water Treat.*, **57**, 10632 (2016); https://doi.org/10.1080/19443994.2015.1040462
44. A. Labidi, A.M. Salaberria, S.C.M. Fernandes, J. Labidi and M. Abderrabba, *J. Taiwan Inst. Chem. Eng.*, **65**, 140 (2016); https://doi.org/10.1016/j.jtice.2016.04.030
45. M.-W. Wan, C.-C. Wang and C.-M. Chen, *Int. J. Environ. Sci. Dev.*, **4**, 545 (2013); https://doi.org/10.7763/IJESD.2013.V4.411
46. M.R. Gopal Reddi, T. Gomathi, M. Saranya and P.N. Sudha, *Int. J. Biol. Macromol.*, **104**, 1578 (2017); https://doi.org/10.1016/j.ijbiomac.2017.01.142
47. O. Rahmani, B. Bouzid and A. Guibadj, *E-Polymers*, **17**, 383 (2017); https://doi.org/10.1515/epoly-2016-0318
48. K. Vijayalakshmi, T. Gomathi, S. Latha, T. Hajeeth and P.N. Sudha, *Int. J. Biol. Macromol.*, **82**, 440 (2016); https://doi.org/10.1016/j.ijbiomac.2015.09.070
49. M.S. Hussain, S.G. Musharraf, M.I. Bhanger and M.I. Malik, *Int. J. Biol. Macromol.*, **147**, 643 (2020); https://doi.org/10.1016/j.ijbiomac.2020.01.091
50. D. Allouss, Y. Essamlali, A. Chakir, S. Khadhar and M. Zahouily, *Environ. Sci. Pollut. Res. Int.*, **27**, 7476 (2020); https://doi.org/10.1007/s11356-019-06950-w
51. C.B. Godiya, X. Cheng, D. Li, Z. Chen and X. Lu, *J. Hazard. Mater.*, **364**, 28 (2019); https://doi.org/10.1016/j.jhazmat.2018.09.076
52. W.S.W. Ngah and S. Fatinathan, *Chem. Eng. J.*, **143**, 62 (2008); https://doi.org/10.1016/j.cej.2007.12.006